Research Guru
Online Journal of Multidisciplinary Subjects (ISSN : 2349-266X)
UGC Approved Journal No. 63726
Impact Factor:4.081
Volume-12, Issue-4, March-2019 www.researchguru.net

A PSEUDOPOTENTIAL STUDY ON THE THERMODYNAMIC AND ELASTIC PROPERTIES OF $Pd_{39}Ni_{10}Cu_{30}P_{21}$ BULK METALLIC GLASS

Alkesh L. Gandhi

Asst. Prof., Department of Physics, B. V. Shah(Vadi-Vihar) Science College,

C. U. Shah University, Wadhwan, 363 002, Gujarat, India,
gandhi.alkesh.jain@gmail.com, (+91)9033096903

Aditya M. Vora

Asso. Prof., Department of Physics, University School of Sciences, Gujarat University, Ahmedabad, 380 009, Gujarat, India *voraam@gmail.com, (+91)9426956016*

ABSTRACT

The study of phonon dynamics of a bulk metallic glass (BMG) based on pseudopotential concept is an effective tool for theoretical revelation of its various properties, which helps in finding its fresh and state-of-the-art applications. The vibrational dynamics of quaternary BMG $Pd_{39}Ni_{10}Cu_{30}P_{21}$ has been theoretically studied in terms of longitudinal and transverse mode of phonon eigen frequencies. The electron-ion interactions are represented by a well-established Shaw's model potential with the two widely accepted local field correction functions viz. Hartree (H) and Taylor (T) under the two comparable approaches suggested by Takeno-Goda (TG) and Bhatia-Singh (BS). Here, pair correlation function (PCF) $g(r)$ is generated theoretically from interatomic pair potential V(r). The computed results of the phonon dispersion curves (PDC) produce respective phononic nature in the amorphous glassy alloy.

KEY WORDS: Bulk metallic glass, Interatomic pair potential, Pair correlation function, Phonon dispersion curve, Thermodynamic properties, Elastic properties.

1. INTRODUCTION:

For decades, metallic glasses have been a field of continued interest due to their unusual properties, unique structure and exciting technological promises. Their properties like high fracture strength, soft magnetism, excellent corrosion and wear resistances, anomalous electronic transport properties make BMGs an inevitable choice for the new engineering materials in several applications extended from the common window glass to sports materials, prosthetic devices, scientific instruments, fashion jewelries, data storage devices in digital media, cellphone case, outer body of space vehicle etc. BMGs are amorphous alloys. They exhibit liquidus temperature below melting points of constituent elements. They behave as an atomically frozen liquid that form glassy solids with a unique amorphous atomic structure having high yield strength and high elastic limit under shock impact conditions as

they lack slips planes. BMGs have been attracting strong interest as they serve to highlight some of the challenging issues waiting for resolutions from the researchers.[1, 2].

The quaternary BMG $Pd_{39}Ni_{10}Cu_{30}P_{21}$ has considerable potential for the investigation of its extraordinary GFA, wide super-cooled liquid regions, highest reduced glass transition temperature; and they can be prepared into glass with a maximum thickness of over 70 mm at a cooling rate less than 1 K/s [3, 4]. It shows increased ductility even by the homogeneous dispersion of spherical pores into glassy matrix. In addition to this increment in ductility, this porous BMG exhibited the falls in Young's modulus, specific weight and strength, as well as increase in absorption energy up to fracture. This BMG has dense random packed atomic configuration. Since the metallic components Pd, Ni and Cu in the BMGs are of FCC (face-centered cubic) structure, it is likely that the atomic configuration in the Pd based BMGs is close to that of the crystalline FCC structure. $Pd_{39}Ni_{10}Cu_{30}P_{21}$ BMG at room temperature up to 23.5 GPa reveals pressure-induced structural relaxation. Progressively elevated pressure gives rise to structural stiffness of the BMG, which results in a smaller pressure dependence of the volumetric change [5]. While transition from glassy state to super cooled liquid and crystalline structure, $Pd_{39}Ni_{10}Cu_{30}P_{21}$ BMG results in formation of coarse-grained spongy structures [6, 7]. Its density, molar mass, glass transition temperature and fragility are 9.152 $g\backslash cm^3$, 72.9 $g/mole$, 586 K and 55 respectively as calculated by Jiang and Dai [8]. Levin *et al.* [9] studied the elastic properties of this BMG at different temperatures and densities using micro-acoustical technique.

In the present computational work, the pseudopotential theory [1, 2] is applied to study the thermodynamic, elastic and some other properties through vibrational dynamics of $Pd_{39}Ni_{10}Cu_{30}P_{21}$ BMG. Its phonon frequencies are obtained using two main computational approaches developed by Takeno-Goda (TG) [10, 11] and Bhatia-Singh (BS) [12, 13]. The screening influence on the properties of $Pd_{39}Ni_{10}Cu_{30}P_{21}$BMG is studied by two local field correction functions viz. Hartree (H) [14] and Taylor (T) [15]. The thermodynamic properties viz. transverse sound velocity (v_T), longitudinal sound velocity (v_L), Debye temperature (θ_D); and also, some elastic properties such as Young's modulus (Y), modulus of rigidity (G), isothermal bulk modulus (B_T), Poisson's ratio (σ) are computed using PDC [1, 2].

The application of pseudopotential to BMGs involve the assumption of 'pseudo-ions' with average properties that replace three types of ions in the BMGs, and the electron gas is supposed to infuse through them. The existence of electron−pseudo-ion is possible due to the pseudopotential and the electron-electron interaction involved through a dielectric screening function.

In the present work, the well successful Pseudo-Alloy Atom (PAA) model [1, 2] is adopted for studying the vibrational properties of $Pd_{39}Ni_{10}Cu_{30}P_{21}$ BMG. The mathematical illumination on Shaw's constant core model potential [16] is,

$$W(q) = -\frac{8\pi Z}{\Omega_0 q^2}\left[\frac{\sin \boldsymbol{q}r_c}{\boldsymbol{q}r_c}\right]. \quad (01)$$

here, **q** is the wave vectors, Z is valence and Ω_0 is atomic volume. The model potential parameter r_C is obtained by fitting either to some experimental data or to realistic form-factors or other data relevant to the properties investigated.

In such computational investigations, the pseudopotential parameter is so fixed that it may generate a PCF accurately harmonized with the experimental data found in the literature. The electron-ion-electron interactions for BMGs can be explained meaningfully PAA model instead of Vegard's law [1, 2].

2. THEORETICAL METHODOLOGY

The quaternary BMG system $A_pB_qC_r\,D_s$ (where p, q, r and s are the proportionate concentration of the concerned element) can be considered to be a multi-component fluid of the bare ions and mixed ions immersed in a uniform electron gas. If the pair potentials of the single components are known, the mean effective density dependent interatomic pair potential V(r) for the BMG system can be explained successfully [17].

In the theoretical analysis for the study of vibrational dynamics of a BMG, the fundamental component pair potential [14, 16, 18] is given by,

$$V(r) = V_s(r) + V_b(r) + V_r(r). \quad (02)$$

The contribution from the s-electron to the pair potential $V_s(r)$ is then,

$$V_s(r) = \left[\frac{{Z_s}^2 e^2}{r}\right] + \left(\frac{\Omega_0}{\pi^2}\right) \int F(q) \left[\frac{\sin(qr)}{qr}\right] q^2\, dq \quad (03)$$

Where, Ω_0 is the effective atomic volume of the mono-component fluid and r is the core radius.

Here, the number of s-valance electron $Z_s \cong 1.5$ is obtained by integrating the partial S-density of states, which result from the self-consistent band structure computation for the entire $3d$ series and $4d$ series,

Z_d is the number of d-electrons contributing to the pair-potential. The d-state radii r_d and the nearest neighbor coordinate number N are given by [1, 2, 19],

$$V_b(r) = -Z_d \left(1 - \frac{Z_d}{10}\right) \left(\frac{12}{N}\right)^{\frac{1}{2}} \left(\frac{28.6}{\pi}\right) \left(2\frac{r_d^3}{r^5}\right) \quad (04)$$

$V_b(r)$ allows the Friedel-model band broadening contribution to the transition-metal cohesion.

$$V_r(r) = Z_d \left(\frac{450}{\pi^2}\right) \left(\frac{r_d^6}{r^8}\right). \quad (05)$$

Here, $V_r(r)$ arises from the repulsion of the d-electron muffin-tin orbitals on different sites due to their non-orthogonality. Wills and Harrison [19] studied the effects of the s-band and d-band.

Where, $f(q)$ is the local field correction function, Z is Valance and ħ is the Plank's constant. m_e and e are mass and charge of an electron respectively

For BMG, the model potential parameter r_c **[1, 2, 19]** is given below.

$$\boldsymbol{r_c} = \left[\frac{(0.51)\, r_S}{(Z)^{1/3}}\right] \quad (06)$$

Where, r_s is the Wigner Seitz radius of the BMG.

The input parameters and constants used for computation are tabulated in **table: 1**.

Table 1: Input parameters for computational study of $Pd_{39}Ni_{10}Cu_{30}P_{21}$ BMG.

Z	Z_S	Z_d	R_d (au)	R_s (au)	Ω_0 $(au)^3$	N_C	M (amu)	r_c (au)
2.92	1.50	7.02	1.63	2.0209	100.95	9.48	72.93	0.7211

The parameters like electron valency Z_s, d-electron valency Z_d, d-band radius r_d and coordination number N are determined from the band structure data of the pure metallic component which are already found in the literature **[1, 2, 19]** and obtained by the following expressions related to PAA model in the pseudopotential theory.

$$Z_d = pZ_{dA} + qZ_{dB} + rZ_{dC} + sZ_{dD} \quad (07)$$

$$Z_s = pZ_{sA} + qZ_{sB} + rZ_{sC} + sZ_{SD} \quad (08)$$

$$r_d = pr_{dA} + qr_{dB} + rr_{dC} + sr_{dD} \quad (09)$$

$$\mathrm{N} = pN_A + qN_B + rN_C + sN_D \quad (10)$$

Z_A, Z_B, Z_c, Z_D and Z is valency with p, q, r and s are the respective concentrations of different elements of the BMG in the form of $A_pB_qC_rD_s$. The PCF $g(r)$ is as important as the pair potential V(r) in studying a BMG **[1, 2, 20]**.

$$g(r) = \exp\left[\left(\frac{-V(r)}{k_BT}\right) - 1\right]. \quad (11)$$

Where, T is Room temperature and k_B, the Boltzmann's constant.

The mathematical notations and theoretical analysis are well discussed in the respective papers of TG- and BS- approaches **[11 – 12, 18, 21 – 23]**. In the long-wavelength limit of the phonon frequency spectrum, the longitudinal and transverse frequencies are proportional to the wave vectors.

$$\therefore \quad \omega_L = \nu_L\, q \quad \text{and} \quad \omega_T = \nu_T\, q. \quad (12)$$

The mathematical expressions of the longitudinal sound velocity ν_L and the transverse sound velocity ν_T ,which are computed from the long-wavelength limits of the PDC, are given in the literatures **[1, 2, 11-13].** Young's modulus Y, Isothermal bulk modulus B_T, Modulus of

rigidity G, Poisson's ratio σ and the Debye temperature θ_D are also computed by the expressions **[1, 2]** given below.

$$B_T = \rho \left[{v_L}^2 - \frac{4}{3} {v_T}^2 \right] \quad (13)$$

$$\mathrm{G} = \rho {v_T}^2 \quad (14)$$

$$\sigma = \frac{1 - 2\left({v_T}^2 / {v_L}^2 \right)}{2 - 2\left({v_T}^2 / {v_L}^2 \right)} \quad (15)$$

$$Y = 2G(\sigma + 1) \quad (16)$$

$$\theta_D = \frac{\hbar \omega_D}{k_B} = \frac{\hbar}{k_B} 2\pi \left[\frac{9\rho}{4\pi} \right]^{1/3} \left[\frac{1}{{v_L}^3} + \frac{2}{{v_T}^3} \right]^{-1/3} \quad (17)$$

Here, ω_D is the Debye frequency, ρ is isotropic number density.

3. RESULTS AND DISCUSSION:

The theoretically computed interatomic pair potentials of $Pd_{39}Ni_{10}Cu_{30}P_{21}$ BMG are shown in **Figure 1** in which the screening dependency is plotted by Pair potential $V(r)$ (Ryd.) versus Interatomic distance r (au).

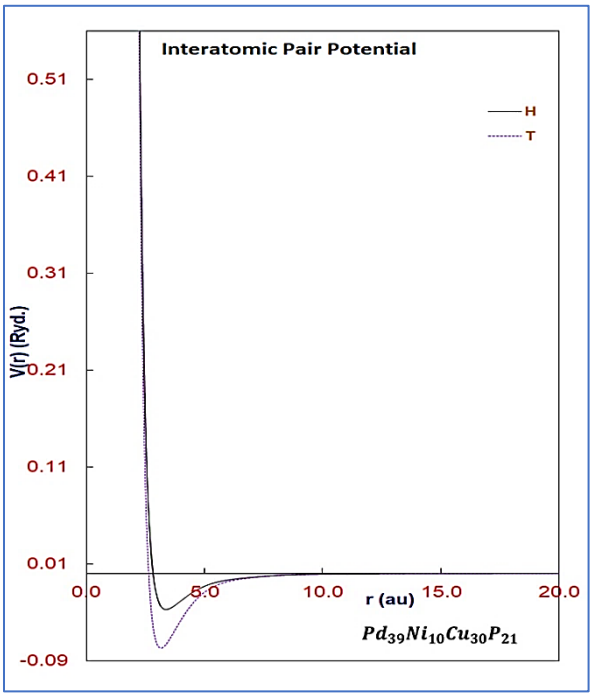

Figure 1: Inter atomic Pair Potentials of $Pd_{39}Ni_{10}Cu_{30}P_{21}$ BMG.

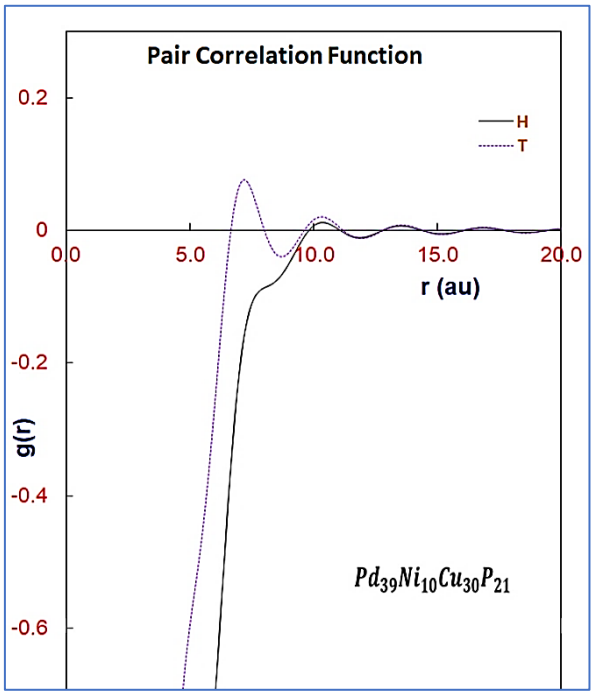

Figure 2: Pair Correlation Function of $Pd_{39}Ni_{10}Cu_{30}P_{21}$BMG

It reveals that the pattern of the interatomic pair potential V(r) is notably changed under exchange and correlation effects in the static H-dielectric screening. The first zero of the interatomic pair potentials $V\ (r = r_0)$, due to both local field correction functions, occurs at $r_0 = 2.7$ au**.** The nature of the screening affects interatomic pair potential V(r), well-width and its minimum position $V(r)_{min}$. The potential depth goes deep with increment of effective volume Ω_0. Various screening functions influence and slightly increase well-depth. In the pair potential, the depth is seen at $r = 3.4\,au$ for H and at $3.2\,au$ for T correction functions. Present results do not show any oscillating behaviour. The potential energy constantly remains negative within the large $r-$ region. Thus, the part of plot showing Coulomb repulsive potential dominates the oscillations due to electron-ion interactions, which gives the negligibly minor waving shape in the interatomic pair potential V(r) after $r = 8.7\ au$. In the attractive part, interatomic pair potentials converge to a finite value instead of being zero. Both interatomic pair potentials display the combined effect of $s-$and $d-$electrons. The repulsive part of the interatomic pair potential $V(r)$ is drawn lower and its attractive part is deeper due to the $d-$electron effect with when the $V(r)$ is shifted towards the lower $r\ -$values. Thus, the derived results seem to support $d-$ electron effect [24].

The plot of pair correlation function $g(r)$ versus interatomic distance r shows the screening effect. For the H- and T- local field correction functions, the nearest neighbouring distance in the form of the 1st peak (r_1) appears at 7.8 and 7.2 au the 1st peak (r_1) respectively, the 1st atomic shell distance as the 2nd peak (r_2) is found at 10.4 and 10.3 au respectively and the 2nd atomic shell distance as the 3rd peak (r_3) occurs at 13.5 and 13.6 au respectively. The mean values of $\langle r_1\rangle, \langle r_2\rangle$ and $\langle r_3\rangle$ are 7.5, 10.35 and 13.55 respectively. For H- and T- screening functions, the ratio of (r_2/r_1) is found 1.33 and 1.43 respectively while the ratio of (r_3/r_1) is found 1.73 and 1.86 respectively. For both local field correction functions, the mean ratio of 2nd to 1st peak is around 1.38, which is nearer to the characteristics for the disordered yet closed pack crystallographic structures and the mean ratio of the 3rd to 1st peak is nearly found 1.80 that suggests incomplete amorphisation of the samples **[24]**. These both ratios suggest that the atomic arrangement of the structure influences the short-range order of nearest neighbours. A large main peak, in the PCF plot, at the nearest-nearest distance is followed by smaller peaks corresponding to some more distant neighbours. It is rather difficult to draw any specific remarks for the disorder after $r\sim$10.1 au because the PCFs using both functions mostly overlap each other from there. The long-range order is normal due to the waving shape of the interatomic pair potential V(r).

The phonon dispersion curves of $Pd_{39}Ni_{10}Cu_{30}P_{21}$BMG was theoretically investigated by Chaudhari *et al*. [25] using a different bare ion model potential formalism by H- and T- local field corrections functions under HB- and BS- approaches. Wang [8, 9] has experimentally studied properties of this BMG using ultrasonic technique.

Figures **3** and **4** show the 'phonon eigen frequencies' for longitudinal and transverse phonon modes, computed with TG− and BS− approaches respectively with H- and T-. screening functions. The obtained vibrational properties based upon pseudopotential theory for this BMG can be compared with the other such [25, 26] and experimentally generated

[9, 27, 28] data available in the literature. The inclusion of exchange and correlation effect increases the phonon eigen frequencies for both longitudinal and transverse modes.

The first minimum for the longitudinal frequency (ω_L) in the TG-approach, is found around $q \approx 2.7$ and 2.9 $Å^{-1}$ for H- and T- screening functions respectively, while in the BS-approach, the same is found around $q \approx 1.7$ for H- function and $q \approx 1.6 Å^{-1}$ for T- function.

Typically, the dispersion relations express a minimum near q_p, the wave-vector where the static structure factor $S(q)$ of the BMG has its first maximum. The first maximum for the longitudinal frequency $(\omega_{L\ max})$ in the TG-approach is found around at $q \approx 1.3$ $Å^{-1}$ for H-function and $q \approx 1.4$ $Å^{-1}$ for T- function. In case of BS-approach, the first maximum for the longitudinal frequency $(\omega_{L\ max})$ is found around $q \approx 0.8$ and 0.7 $Å^{-1}$ for H- and T-local field correction functions respectively.

In TG approach, the first minimum transverse frequency $(\omega_{T\ min})$ is found at $q \approx 4.0$ and 4.2 $Å^{-1}$ respectively for the H- and T- screening functions. In the BS approach, the same is found at $q \approx 1.6$ $Å^{-1}$ for both functions. For the transverse branch $(\omega_{T\ max})$, the first maximum is found around at $q \approx 2.6$ and 2.8 $Å^{-1}$ for H- and T- local field correction functions in TG- approach. Similarly, in BS approach, the first maximum for the transverse branch $(\omega_{T\ max})$ is found at ≈ 1.0 $Å^{-1}$ for both functions.

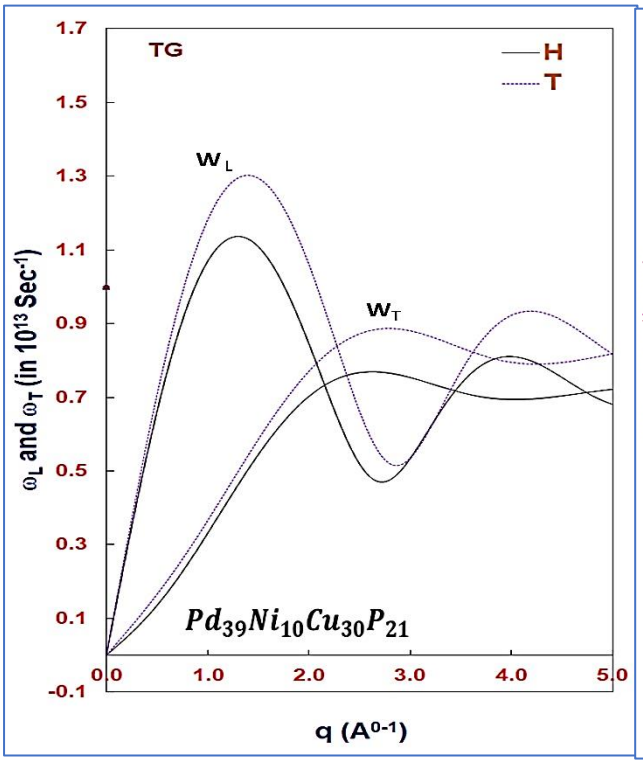

Figure :3
Longitudinal and Transverse Phonon frequencies (ω_L and ω_T) For $Pd_{39}Ni_{10}Cu_{30}P_{21}$ BMG using TG approach.

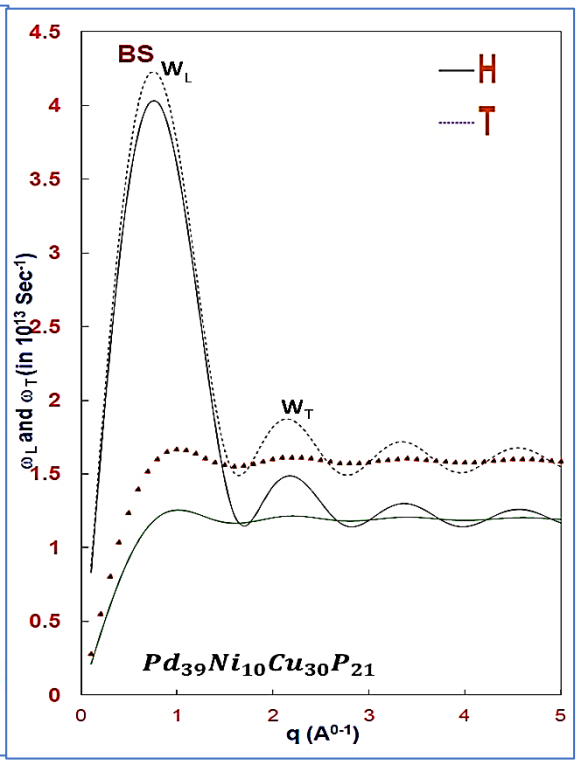

Figure :4
Longitudinal and Transverse Phonon frequencies (ω_L and ω_T) For $Pd_{39}Ni_{10}Cu_{30}P_{21}$ BMG using BS approach.

The first crossover position of ω_L and ω_T in the TG-approaches is seen at $q \approx 2.2$ and 2.3 $Å^{-1}$ for H and T- functions respectively. In the BS approach, nothing can be stated about the crossover positions of ω_L and ω_T as it is vague due to major overlapping on each other so, nothing can be obtained from this plot. In the transverse branch of BS approach, the frequencies increase with the wave vector **q** and then saturates at $\mathbf{q} \approx 1.0\ Å^{-1}$ and that supports the famous Thorpe model **[29]** in which, it is shown that a solid glass contains finite liquid clusters. The transverse phonons are absorbed for such frequencies as they are larger than the smallest eigen frequencies of the largest cluster.

The plotted phonon dynamical graphs of $Pd_{39}Ni_{10}Cu_{30}P_{21}$ BMGs for both, TG- and BS-models given by **figures 3** and **4** respectively disclose that the longitudinal mode oscillations are more prominent than that of the transverse one. The instability of the transverse mode oscillations is because of anharmonicity of the atomic vibration in the BMG system. The collective excitations at larger momentum transfer is because of the prominence of longitudinal mode vibrations only.

Table 2 : Elastic and Thermodynamic properties of $Pd_{39}Ni_{10}Cu_{30}P_{21}$ BMG.

Approach.	Scr. Fn.	$v_L \times 10^5\ cm/s$	$v_T \times 10^5\ cm/s$	$B_T \times 10^{11}\ dyne/s^2$	$G \times 10^{11}\ dyne/s^2$	σ	$Y \times 10^{11}\ dyne/s^2$	θ_D K
TG	**H**	1.2825	0.2356	1.2713	0.0449	0.4825	0.1332	32.57
	T	1.3645	0.3156	1.3995	0.0806	0.4717	0.2372	43.58
BS	**H**	5.0254	1.2916	18.6402	1.3502	0.4646	3.9551	178.23
	T	5.3023	1.7071	19.6099	2.3587	0.4422	6.8034	234.94
Others (Theoretical Data)	[25]	3.40 3.82 4.72	1.96 2.20 1.95	7.143 11.21 16.0	3.571 4.483 3.317	0.25 0.397	8.928 8.967 9.266	274.86 307.96 300.54
	[25]	---	---	15.91	3.51	---	---	---
	[26]	4.750	1.963	15.94 15.91 15.87 15.85	3.53 3.51	0.399 0.397	9.86 9.82 9.81	279.60 280.00
Experimental data.	[9]	3.90 4.71 4.97 5.00 5.02	1.87 1.89 1.93 1.95 2.03	9.200 14.869 17.67 18.122 18.363	3.137 3.434 3.461 3.505 3.691	0.34 0.39 0.41	---	---
	[27]	4.75	1.963	15.94	3.53	0.397	9.85	280.00
	[28]	4.74	1.96	15.91	3.51	0.40	9.82	280.00

The theoretically generated elastic and thermodynamic properties from the elastic part of $Pd_{39}Ni_{10}Cu_{30}P_{21}$ BMG are given in **table 02.** The screening function S influences more on the results of v_L and v_T than the rest in this group. The comparison of other such available

theoretical [25, 26] and experimental results [9, 27, 28] supports this computational work up to the most extent and proposes for the proper dielectric screening as an important part to explain desired properties of $Pd_{39}Ni_{10}Cu_{30}P_{21}$ BMG. The results generated by the BS-approach are higher than those obtained by the TG-approach and best matches with the experimental data. The present study successfully represents that, the proposed (Shaw's) model potential is one of the best suitable to study of phonon dynamics of this one and many other such BMGs, where the influences of various local field correction functions are observed.

4. CONCLUSION:

Summing up this investigative study, it is concluded that the phonon dynamics of a BMG can be estimated by TG- and BS- approaches with the successful application of the Shaw's model potential by supporting the present approach of PAA to provide important information of the BMG system. The dielectric function is significant in the computation of the screening potential due to electron gas, and the local filed correction functions due to H- and T- are used in such observations. The relative effects of exchange and correlation in the selected properties are examined by H- and T- different local field correction functions, which show substantial variations according to vibrational properties. The computed PDCs show extensive features of broad range collective excitations in $Pd_{39}Ni_{10}Cu_{30}P_{21}$ BMG and they are consistent with the other such and experimental data. The thermodynamic properties obtained due to BS-approach are higher than those due to TG-approaches. The calculated results of the BS approach are in excellent agreement with the experiment data compared to the TG-approach. The complete picture divulges the importance of local field correction function as well as the approaches in analysing the important properties of the BMG.

References:

[1] A. M. Vora, Vibrational Dynamics of Binary Metallic Glasses, Lap Lambert Academic Publishing, Germany (2012).

[2] A.M. Vora, Vibrational Dynamics of Bulk Metallic Glasses Studied By Pseudopotential Theory, Computational Materials, Ed. Wilhelm U. Oster, Nova Science Publishers, Inc., New York (2009), pp.119-176.

[3] A. Inou, Mater. Trans., JIM, Vol. 37, (1996), p.1531.

[4] A. Meyer, R. Busch and H. Schober, Phy. Rev. Lett., Vol. 83, (1999), p. 5027.

[5] L. M. Wang, Z. J. Zhan, J. Liu, L.L. Sun, G. Li and W. K. Wang, Journal of Physics: Condensed Matter, Vol. 13, (2001), pp. 5743–5748

[6] V. M. Levin, J. S. Petronyuk, L. Wang and J. Hu, Mat. Res. Soc. Symp. Proc., Materials Research Society, (2003), p. 754

[7] L. M. Wang, G. Li, Z. J. Zhan, L.L. Sun and W. K. Wang, Philosophical Magazine Letters, Vol. 6-81, (2001), pp. 419 – 423.

[8] M. Jiang and L. Dai, Intrinsic correlation between fragility and bulk modulus in metallic glasses, (2007), Physical Review B, vol. 76, pp. 054204:1-7. DOI: 10.1103/PhysRevB.76.054204.

[9] V. M. Levin *et al.*, (2003), Mat. Res. Soc. Symp. Proc., pp. 1.18.1-6

[10] S. Takeno; M. Goda, Prog. Thero. Phys., (1971), Vol. 45, pp. 331-352.

[11] S. Takeno; M. Goda, Prog. Thero. Phys., (1972), Vol. 47, pp. 790-806.

[12] A. B.Bhatia; R.N. Singh, Phys. Rev B., (1985), Vol. 31, pp. 4751-4758.

[13] M. M. Shukla; J. R. Campanha, Acta Phys. Pol. A., (1998), Vol. 94, pp. 655-660.

[14] W. A. Harrison, Elementary Electronic Structure, (1999), World Scientific, Singapore.

[15] R. Taylor, J. Phys. F: Met. Phys., (1978), Vol. 8, pp. 1699-1702.

[16] R.W.Shaw, Phy. Rev., (1968), Vol. 174, p. 769.

[17] Gupta A.; Bhandari D.; Jain K. C.; Saxena N. S. Phys. Stat. Sol. (b). Vol. 95, (1996), pp. 367-374.

[18] W. A. Harrison, Pseudopotentials in the Theory of Metals, (1966), W. A. Benjamin, Inc., New York.

[19] J. M. Wills; W.A. Harrison, Phys. Rev B., (1983), Vol. 28, pp. 4363-4373.

[20] E. TFaber, Introduction to the Theory of Liquid Metals; (1972), Cambridge Uni. Press: London.

[21] V. Heine and D. Weaire, Solid State Physics 24, Eds. H. Ehrenreich, F. Seitz and D. Turnbull, Academic Press, New York (1970) p.249.

[22] L. I. Yastrebov and A. K. Katsnelson, Foundations of One-Electron Theory of Solids, (1987), Mir Publications, Moscow.

[23] J.M. Ziman, Principal of the theory of the solids, 2nd edition, (1972), Cambridge Uni. Press, London.

[24] L.D. Sulir, M.Pyka and A. Kozlowski, Acta Phys. Pol. A. (1983), Vol. 63, pp. 435-443

[25] P. Chaudhari *et al.*, Int. Conf. on Rec. Trends in App. Phy. & Mat. Sc., A.I.P. 1536, (2013), pp. 635-636. DOI:10.1063/1.4810387.

[26] W. H. Wang, The elastic properties, elastic models and elastic perspectives of metallic glasses, Progress in Material Science, (2012), Vol. 57, pp. 487-656

[27] W. K. Wang, Materials transactions : Bulk metallic glasses-III, Vol. 42 (4), (2001), pp. 606-612.

[28] W. H. Wang, F. Y. Li, M. X. Pan, D. Q. Zhao and R. J. Wang, Acta Materialia, (2004), Vol. 52, pp. 715-719.

[29] M. F. Thorpe, J. Non-Cryst. Sol. (1983), Vol. 57, pp.355-370.